NJC
New Journal of Chemistry
A journal for new directions in chemistry

Accepted Manuscript

This article can be cited before page numbers have been issued, to do this please use: A. Basu, A. Mahammmad and A. Das, *New J. Chem.*, 2022, DOI: 10.1039/D1NJ06007D.

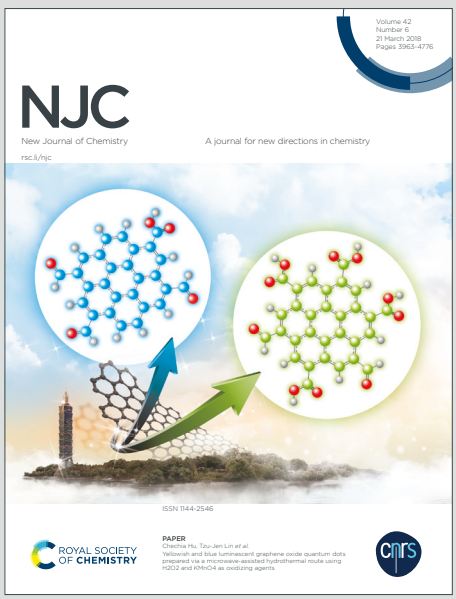

This is an Accepted Manuscript, which has been through the Royal Society of Chemistry peer review process and has been accepted for publication.

Accepted Manuscripts are published online shortly after acceptance, before technical editing, formatting and proof reading. Using this free service, authors can make their results available to the community, in citable form, before we publish the edited article. We will replace this Accepted Manuscript with the edited and formatted Advance Article as soon as it is available.

You can find more information about Accepted Manuscripts in the Information for Authors.

Please note that technical editing may introduce minor changes to the text and/or graphics, which may alter content. The journal's standard Terms & Conditions and the Ethical guidelines still apply. In no event shall the Royal Society of Chemistry be held responsible for any errors or omissions in this Accepted Manuscript or any consequences arising from the use of any information it contains.

REVISED MANUSCRIPT

Inhibition of the formation of lysozyme fibrillar assemblies by the isoquinoline alkaloid coralyne†

Anirban Basu* Adil Mahammad and Arindam Das

Department of Chemistry, Vidyasagar University, Midnapore 721 102, India

Corresponding Author

Dr. Anirban Basu, Ph.D

Department of Chemistry, Vidyasagar University, Midnapore 721 102, India

e-mail: anirbanbasu@mail.vidyasagar.ac.in/basu.ani.anirban@gmail.com

† Electronic supplementary information (ESI) available: Fig. S1 and S2. See DOI:

REVISED MANUSCRIPT

View Article Online
DOI: 10.1039/D1NJ06007D

Abstract

Protein aggregation into oligomeric and fibrillar species are the hallmark of many degenerative diseases like Alzheimer's and prion diseases, as well as type II diabetes. Compounds that can modulate protein aggregation or disintegrate the preformed fibrils can serve as potential drug candidates for the remedial treatment of aggregation diseases. In present study we have examined the anti-amyloidogenic potency of the synthetic isoquinoline alkaloid coralyne by employing various spectroscopic and imaging approaches. The kinetics of amyloid fibrillation by chicken egg-white lysozyme (HEWL) and the anti-amyloidogenic influence of coralyne on the fibrillogenesis process were studied using thioflavin T assay. The kinetics of HEWL fibrillation were significantly modulated in presence of coralyne. We have demonstrated that coralyne significantly inhibits the fibrillation of HEWL. A complementary Congo red assay in absorbance was also performed to reaffirm the fibril inhibition propensity of coralyne. The changes in surface hydrophobicity of the protein upon fibrillation were monitored by nile red assay. The steady-state fluorescence studies, anisotropy measurements and circular dichroism measurements collectively confirm the attenuation of the amyloid fibrils in the isoquinoline alkaloid coralyne. Atomic force microscopic imaging suggested that the fibrillation was reduced in presence of coralyne and the fibrils formed were also less matured. The complete binding thermodynamics was also elucidated using microcalorimetry and docking studies lend insights into the type of forces governing the binding interaction. Since lysozyme is an important model system for studying

protein aggregation, the synthetic isoquinoline alkaloid coralyne can serve as a promising model compound for the treatment of amyloidosis.

Introduction

View Article Online
DOI: 10.1039/D1NJ06007D

Type II diabetes, Parkinson's disease, transmissible spongiform encephalopathies, Huntington's disease, and Alzheimer's disease, are a group of amyloid diseases where extracellular insoluble deposits are formed in different tissues and organs.[1-5] These extracellular insoluble aggregates are known as amyloid fibrils. X-ray diffraction studies have indicated that the amyloid fibrils possess characteristic β-rich structure where the polypeptide chains form β-strands that are perpendicular to the fibrillar long axis and the inter chain hydrogen bonding that imparts stability to the β-strands are oriented parallel to the same axis and β-sheets running in the direction of the fibrils.[6-8] Since extracellular accumulation of amyloid fibrils in organs and tissues is the characteristic feature of amyloidosis so a comprehensive knowledge of the mechanism underlying fibrillation along with the possible means of its inhibition have received a lot of interest recently.[9-11] Aggregation of proteins is associated various human pathological conditions[12] and hence from a biomedical point of view, suppression of protein aggregation is a major priority in the public health sector. Presently, effective therapeutics for amyloidosis are still obscure as most of the potential anti-amyloidogenic drugs have failed at different stages of clinical trials but the design and identification of organic molecules that suppress fibrillation of amyloidogenic proteins is an area of promising research.[13-15]

Although amyloid fibrillation is associated with various diseases but still amyloid fibrils has been observed in various self-assembling nonpathogenic proteins such as serum albumins and chicken egg-white lysozyme under suitably modified conditions which has led to the belief that amyloidosis is a generic property of the

View Article Online
DOI: 10.1039/D1NJ06007D

polypeptide chains.[16,17] This knowledge is an important step in understanding the mechanisms underlying fibrillogenesis as well as the possible ways to disrupt this process. The knowledge that aggregation is an inherent property of proteins/peptides has led to the belief that there may be common inhibitors for amyloid fibrillation. Natural as well as synthetic small molecules capable of inhibiting fibrillation of various proteins/peptides are known.[18-22]

Lysozyme is basically *N*-acetylmuramide glyconohydrolase which is a monomeric globular protein with 129 amino acid residues. It is found abundantly in various animal protective secretions and lymphatic tissues. It can cause damage to the bacterial cell walls thereby providing protection from bacterial infections. It is even employed as a food preservative as well as an antimicrobial agent.[23-25] Lysozyme is a preferred candidate to study protein folding and dynamics, ligand interactions and amyloid fibrillation because it is stable, naturally abundant and also has drug binding properties.[26-29] It consists of six tryptophan (TRP) and three tyrosine (Tyr)residues as well as four cross-linked disulfide bonds including multitude of α-helices, β-sheets, turns, and loops.[28,30] Active site of lysozyme has a deep crevice which divides it into two domains that are interconnected via an α-helix. One of the domains (amino acids 40-85) has mainly β-sheet conformations while the other domain (amino acids 89-99) is mainly α-helical.[31] Crystal structure of the lysozyme has revealed that TRP-62, 63, and 108 residues are situated near its ligand binding site.[32]

Alkaloids are important nitrogen-containing bases which are produced by plants at the time of metabolism. Alkaloids have an indispensable importance in medicinal

chemistry. Protoberberine alkaloids, an important class of isoquinoline alkaloids, has received lot of attention because they are the active constituents of folk medicines used for centuries. Coralyne (Fig. 1) is an important member of the protoberberine family that has a planar crescent-shaped structure with dibenzoquinolizinium skeleton. It posesses diverse biological properties ranging from antimicrobial, anti-inflammatory, antimalarial, antisecretory, to antileukemic activity and it acts as a dual poison of topoisomerases I and II.[33-36] It has less toxicity but very high antitumor potential.[33,37,38] The nucleic acid binding properties of coralyne are also well documented.[36,38-54] However, the anti-amyloid potential of these alkaloids including coralyne is still unexplored.

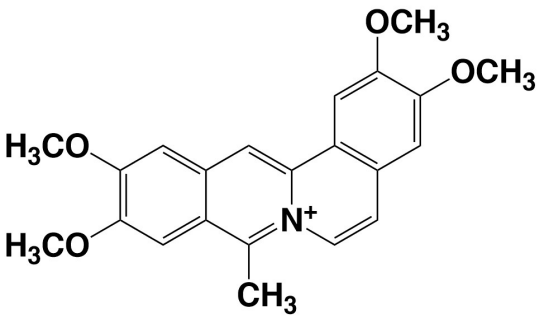

Fig. 1. Molecular structure of coralyne.

Chicken egg-white lysozyme (HEWL) is sequentially homologous (~60%) with human lysozyme, which is associated with hereditary non-neuropathic systemic amyloidosis.[55,56] Therefore, in this work we have investigated the anti-amyloid potential of coralyne using HEWL as a model protein system.

Experimental

Materials

View Article Online
DOI: 10.1039/D1NJ06007D

HEWL, Coralyne chloride (COR), Thiofalvin T (ThT), Congo Red (CR), Nile Red (NR), 8-anilino-1-naphthalenesulfonic acid (ANS), were purchased from Sigma-Aldrich Corporation (St. Louis, MO, USA). All the buffer components were of analytical grade. All the solutions were prepared in deionized Milli-Q water. The fibrils were prepared in glycine-HCl buffer of pH 2.20 containing 100 mM sodium chloride and 1.54 mM sodium azide. HEWL was purified as per the standard protocol[57] while COR was used as recieved. The concentration of COR was determined using molar absorption coefficient value of 14,500 $M^{-1}cm^{-1}$ at 421 nm.[47]

HEWL fibrils preparation

100 mg HEWL was dissolved in freshly prepared 10 mL glycine-HCl buffer of pH 2.20. 2 mL of HEWL stock solution was diluted ten folds with the glycine-HCl buffer and stirred at 60 ^{o}C with polytetrafluoroethylene coated stirring bars (200 rpm).[5,58,59]A similar solution containing 25 µM COR was simultaneously prepared and stirred maintaining identical conditions. At desired time intervals 1 mL aliquots of both the solutions were withdrawn and stored for the subsequent experiments.

Instruments and Methods

The fluorescence experiments like ThT assay, NR assay, ANS assay and intrinsic fluorescence experiments were performed on a Shimadzu RF5301 PC spectrofluorimeter (Shimadzu Corporation, Kyoto, Japan) while the steady state anisotropy experiments were performed on a Quanta Master 400 unit (Horiba PTI, Canada) controlled with FelixGX spectroscopy software. For ThT assay a stock solution of ThT was prepared at first and its concentration was determined following the protocols reported earlier.[5,60] Thereafter, 150 mL of aliquots taken out

View Article Online
DOI: 10.1039/D1NJ06007D

at varying time intervals were diluted with 600 mL glycine-HCl buffer and ThT was added to it so that the final concentration of ThT was 25 μM. The resulting mixtures were incubated in dark for 1 h and then their fluorescence was noted at 485 nm after exciting them at 440 nm.

For NR assay at first a stock solution of 1 mM NR was prepared in DMSO and then 50 mL aliquots withdrawn at various time intervals were diluted to 750 mL with buffer followed by addition of the stock NR solution so that its final concentration was 1 μM. The fluorescence of the resulting mixtures after incubation in dark for 30 mins was noted at the corresponding emission maxima by exciting them at 550 nm.

For ANS assay an aqueous ANS stock solution was prepared and then 50 mL aliquots withdrawn at varying time intervals were diluted to 750 mL followed by addition of ANS stock solution so that its final concentration was 25 μM and the solutions were incubated in dark for 30 mins. Thereafter, the emission spectra were recorded in the 400-600 nm wavelength region after exciting at 370 nm.

For intrinsic fluorescence studies 50 μL aliquots withdrawn at varying time periods were diluted with 700 μL buffer and the fluorescence at the emission maxima was recorded by exciting the solutions at 295 nm.

For steady-state anisotropy experiments 25 μL aliquots were diluted with 725 μL buffer and properly homogenized. Then the anisotropy values were determined at the emission maxima by exciting the solutions at 295 nm.

CR assay was performed on a Jasco V660 spectrophotometer (Jasco International Co, Hachioji, Japan). For CR assay a stock solution of 1 mM CR was prepared in DMSO and then 50 μL aliquots were diluted with 1 mL buffer followed by addition of CR

View Article Online
DOI: 10.1039/D1NJ06007D

from the stock solution. The absorbance of the solutions after incubation for 30 min at the maxima was noted.

Circular dichroism (CD) experiments were performed on a Jasco J815 unit in 1mm path length quartz cuvettes. 100 µL aliquots were diluted three folds with the buffer and thoroughly homogenized and the CD spectra was recorded in 190-250 nm wavelength region. The CD spectra were deconvoluted using the "CONTINLL" analysis program available at DICHROWEB while set 4 was used as the reference.[61-65]

Atomic force microscopy (AFM) experiments were carried out on a Pico plus 5500 ILM AFM (Agilent Technologies, USA) having piezo scanner of maximum range 9 µm. The samples were diluted 100 times with autoclaved Milli-Q water and then 5 µL of the resulting solution was placed on a on a freshly cleaved muscovite Ruby mica sheet and dried completely under vacuum in inert atmosphere. Then the images were taken and subsequently processed using Picoview version 1.1 software and Pico Image Advanced version.

Differential scanning calorimetry (DSC) and isothermal scanning calorimetry (ITC) experiments were performed on a MicroCal VP DSC and ITC units, respectively (MicroCal, Inc., Northampton, MA, USA) following the procedures described in details earlier.[66-73]

Molecular docking analysis has been performed employing the AutoDock 4.2.6 implemented with a Lamarckian genetic algorithm (LGA) to get a thorough insight into the binding site of COR (ligand) on HEWL protein.[74] The three dimensional structure of HEWL was downloaded from RCSB Protein Data bank (PDB ID: 1DPX).

View Article Online
DOI: 10.1039/D1NJ06007D

The spatial data file of COR was downloaded from zinc database (ID ZINC625876) and it was used in docking as a ligand without any further modification. Before starting the docking process, polar hydrogen atoms and Kollman charges were added to HEWL and to avoid hindrance during docking, the water molecules were removed using AutoDock tools. For flexible rotation, the macromolecule was set to be rigid so that the ligand may achieve suitable binding conformation and to estimate these binding conformations Lamarckian genetic algorithm was selected for accomplishing docking. The dimension of the grid box along X, Y, Z axis was set at 94 × 96 × 102 respectively with a grid point spacing of 0.631 Å. The number of Genetic Algorithm Runs was set at 50 and was performed with each run comprising of a population size of 15 individuals and 2,500,000 energy evaluations. The binding conformer was visualized in 2D form by using BIOVIA Discovery Studio Program. Accessible surface areas (ASAs) of HEWL protein in native and complexed form with COR were obtained using an online server available from the Center for Informational Biology, Ochanomizu University.[75] The best docked conformation with lowest binding energy was chosen to analyze the difference in ASA.

Statistical Analysis. The data represented here are mean ± standard deviation of four independent determinations.

Results and Discussion

ThT Assay

The formation of fibrillar assemblies was monitored at low acidic pH and elevated temperature under vigorously agitated conditions by examining both the ultra-structural characteristics of the HEWL samples. ThT being a histochemical dye

capable of staining amyloid aggregates is widely used as a standard extrinsic probe for monitoring the growth of amyloid fibrils.[76] The kinetics of fibrillogenesis were studied both in the absence and presence of COR by observing the evolution of ThT fluorescence with time. ThT shows weak fluorescence in aqueous acidic buffer but its fluorescence increases several folds upon binding with linear array of β-strands. On association with ordered aggregates of HEWL ThT emits high fluorescence which can be used as a key index for studying the fibrillation kinetics. In the absence of COR the ThT fluorescence of HEWL at 485 nm followed a typical nucleation-dependent pathway (Fig. 2A). The plot of ThT fluorescence vs time was sigmoidal in nature with a well defined lag phase where no change is fluorescence was observed followed by an elongation phase where there was a rapid and significant enhancement in ThT fluorescence and finally an equilibration phase where again the fluorescence was virtually unaltered. The nucleation phase for HEWL samples in absence of COR lasted for 4.5 h whereas the growth phase was observed between 5 to 7 h and thereafter there was a saturation phase with marginal changes in fluorescence indicating completion of fibrillogenesis process. In presence

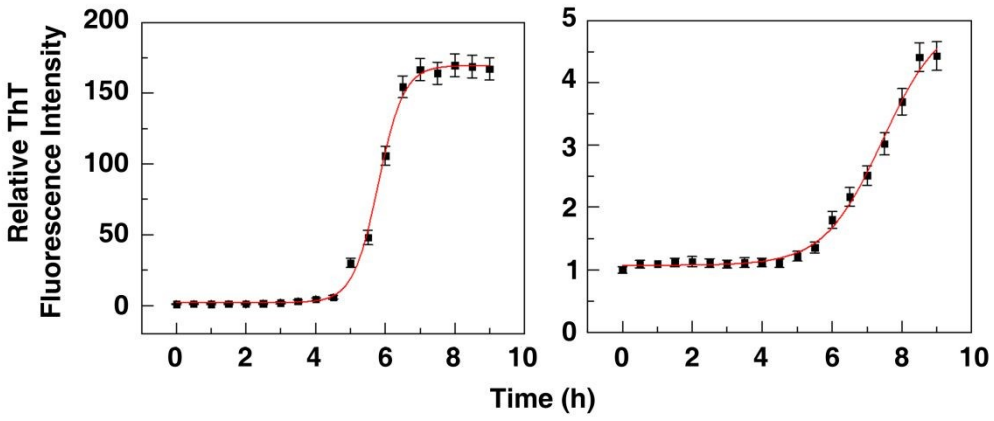

Fig. 2. Variation of the ThT fluorescence intensity at 485 nm with time for HEWL samples in the (A) absence and (B) presence of COR.

of COR the nucleation phase duration was increased till 5.5 h while the growth phase lasted between 6 to 8 h (Fig. 2B). The ThT fluorescence after corrections for inner filter effects[77,78] were fitted to the sigmoidal plot which can be represented by the equation[79]

$$F = F_{min} + \left(\frac{F_{max}}{1 + e^{-\left[\frac{\{t - t_0\}}{\tau}\right]}}\right) \qquad (1)$$

where F, F_{min} and F_{max} denote the fluorescence at time t, initial time and equilibration phase, respectively. t and t_0 are the time of incubation and the time needed to reach 50% of the fluorescence maximum, respectively. The first order aggregation constant (τ) was determined by nonlinear regression whereas the apparent growth rate constant (k_{app}) and lag phase time were determined using the relationships $1/\tau$ and $t_0 - 2\tau$, respectively. The initial nucleation phase was determined to be (5.07 ± 0.06) and (5.77 ± 0.07) h, respectively, in the absence and presence of COR. The t_0 value was determined to be (5.80 ± 0.10) and (7.45 ± 0.13) h, respectively, in the absence and presence of COR. The value of k_{app} was calculated to be (2.73 ± 0.08) and (1.19 ± 0.03) h^{-1}, respectively, in the absence and presence of COR. Hence, every individual act of the fibrillation process was retarded/suppressed in presence of COR. Moreover, COR delays fibrillation by elongation of the initial nucleation phase, an early step in the fibrillogenesis process, whereby the non-amylodogenic conformations in HEWL are stabilized through COR-HEWL complexation.[80,81] The length of the elongation phase is substantially reduced in the presence of COR. The inhibitory influence of COR on HEWL fibrillation was quantified using the equation

View Article Online
DOI: 10.1039/D1NJ06007D

$$\%\ \text{reduction in ThT fluorescence} = \frac{F_o - F}{F_o} \times 100\% \qquad (2)$$

where, F_o and F are the ThT fluorescence intensities of HEWL fibrils in the absence and presence of COR after 9 h of incubation. The inhibitory influence of COR on the formation of HEWL fibrils was envisaged to be around 97% after 9 h. This remarkable attenuation in fibrillogenesis in the presence of COR can be interpreted in terms of the association between COR and the partly unfolded aggregation-prone form of HEWL generated during the initial nucleation phase via a multitude of weak non-covalent interactions. The complexation prevents the hydrophobic portions of the partly unfolded HEWL to interact amongst themselves which results in reduction of the aggregation of the partly unfolded HEWL thereby leading to the inhibition of fibrillation.[82-84] So, we can infer that COR had a remarkable inhibitory influence on the entire process of HEWL fibrillation.

CR Assay

CR is a known histological dye capable of detecting the formation of amyloid fibrils. Amyloid deposits show apple-green birefringence when stained with CR under the cross polarized light.[85,86] Additionally, binding of CR to amyloid fibrils caused an increase in absorbance of the maximum at 542 nm.[86,87] The absorption spectra of HEWL samples stained with CR before and after fibrillation both in the absence and presence of COR is depicted in Fig. 3. The CR absorbance spectra (curve 1, Fig. 3) exhibited a peak at 493 nm but the HEWL fibrillar species incubated with CR showed a red shift of the absorption spectra (curve 2, Fig. 3). A well-defined maximum was observed at 542 nm with concomitant enhancement in absorbance

suggesting the formation of β-sheet-rich, ordered fibrillar assemblies. CR absorbance of HEWL samples treated with COR showed reduced absorbance with a

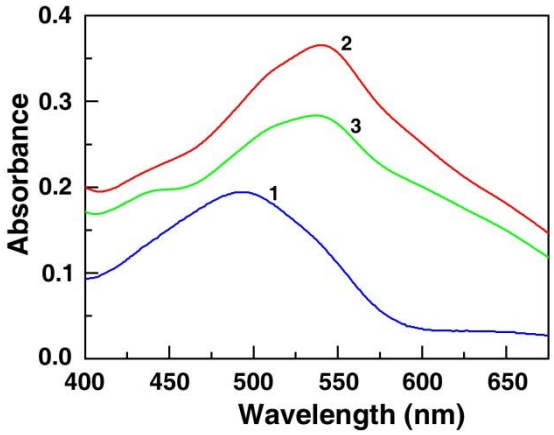

Fig. 3. Absorbance spectra of CR before (curve 1) and after (curves 2 and 3) fibrillation. Curves 2 and 3 represent the CR absorbance spectra of HEWL fibrils after 9 h in the absence and presence of COR, respectively.

blue-shift of the maximum to 537 nm (curve 3, Fig. 3) signifying a reduction in amyloid fibrillar species formation that has cross β-pleated sheet morphology. Hence, both ThT and CR assay revealed that COR had an inhibitory effect on every step of the fibrillation process. An overall reduction of ~22% in absorbance was observed after 9 h of incubation in presence of COR (Fig. 4). Therefore, ThT fluorescence assay in conjunction with CR assay testified that COR exerted a significant attenuating effect on the fibrillogenesis of HEWL.

REVISED MANUSCRIPT

View Article Online
DOI: 10.1039/D1NJ06007D

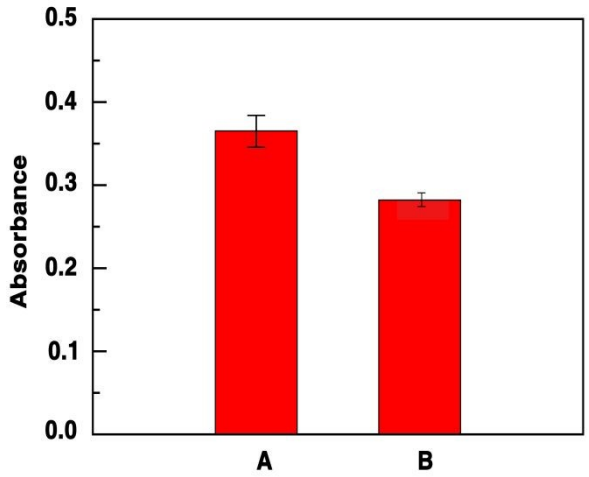

Fig. 4. Difference in CR absorbance after 9 h for HEWL samples in the (A) absence and (B) presence of COR at 542 nm.

NR Assay

Surface hydrophobicity can often act as a gauge for monitoring the tertiary structural changes in HEWL. Monitoring the fluorescence evolution of NR at the corresponding emission maxima against time during the incubation process can yield information about the tertiary structural changes in HEWL during fibrillation. NR is a lipophilic fluorescent dye that is widely used to monitor the microenvironmental changes in biomolecules.[88] Fig. 5 depicts the variation of normalized NR fluorescence at the emission maxima against time. Initially, the HEWL samples in absence of COR showed no noticeable increase in the first 4.5 h accompanied by a marked increase from 5 to 6.5 h of incubation, and thereafter reaching an equilibration plateau after 7 h. In presence of COR, there was noticeable change in NR fluorescence upto 5.5 h followed by a significant increase between 6 to

View Article Online
DOI: 10.1039/D1NJ06007D

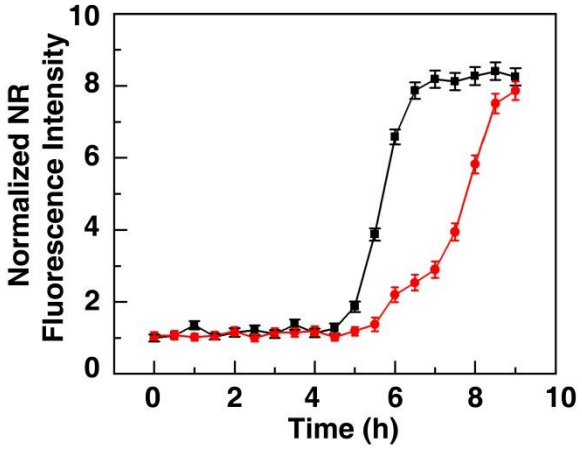

Fig. 5. Variation of the fluorescence intensity of NR at the emission maxima with time for HEWL samples in the absence in the absence (■) and presence (•) of COR.

8.5 h of incubation. Thus, the changes in microenvironment of HEWL accompanying the fibrillation process were retarded in presence of COR. Additionally, a blue-shift in the emission maximum (λ_{max}), indicative of theexposure of buried hydrophobic patches, was observed prior to the increase in NR fluorescence. The variation of NR λ_{max} against time is depicted in Fig. S1.The λ_{max} of NR blue shifted from around 655 to 615 nm in the absence of the COR. Initially, there was no shift in NR λ_{max} upto 4 h and then there was a rapid blue shift between 4 to 5 h and thereafter it reached reached a plateau. This suggested that λ_{max} shift is more sensitive to the tertiary structural changes of HEWL compared to NR fluorescence evolution and blue shift of λ_{max} precedes than the rise of the NR fluorescence emission. In presence of COR the λ_{max} did not exhibit any significant alterations before 4 h of incubation. Thereafter, there was blue shift of λ_{max} from ~653 to ~640 nm between 4.5 to 6 h followed by an equilibration plateau. Thus, there was marked decrease in the extent of blue shift of NR λ_{max} upon addition of COR indicating that the changes in the tertiary structure of HEWL upon fibrillation were arrested in presence of COR. The

View Article Online
DOI: 10.1039/D1NJ06007D

significant reduction in the extent of shift of NR λ_{max} in the presence of COR in comparison to the control is suggestive of the suppression of the changes in surface hydrophobicity of HEWL and retention of the native structure of HEWL. Since microenvironmental changes and changes in surface hydrophobicity are closely associated with the fibrillation process therefore significant attenuation of these changes in presence of COR suggests COR had a significant inhibitory effect on the overall fibrillation process.

ANS Assay

ANS has high affinity for the hydrophobic patches present in HEWL. ANS can bind to the fibrillar species of HEWL resulting in marked enhancement of the intensity of fluorescence along with a blue shift of the emission maximum from

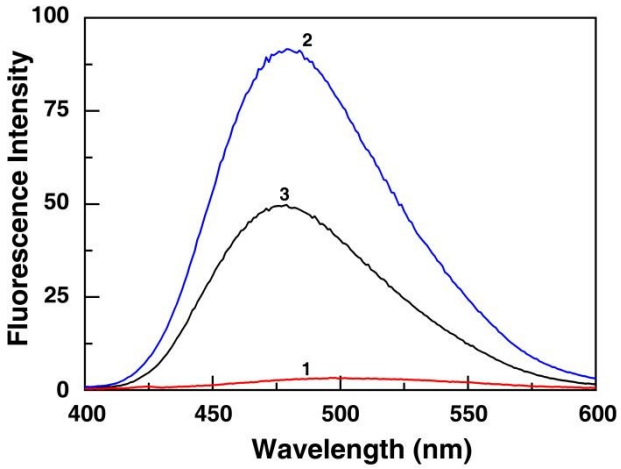

Fig. 6. ANS fluorescence spectra of HEWL samples before (curve 1) and after fibrillation (curves 2 and 3). Curves 2 and 3 represent the ANS fluorescence spectra of HEWL fibrils in the absence and presence of COR, respectively.

around 510 to 480 nm.[89,90] Before the commencement of amyloid fibrillation conformational changes take place in HEWL which leads to the exposure of accessible hydrophobic regions in HEWL. Thus, monitoring the degree of hydrophobic exposure can serve as an useful tool for studying the fibrillation

process.[82,91-93] In acidic aqueous buffer ANS is weakly fluorescent with an emission maximum centered at 513 nm but the fluorescence intensity of ANS showed a prominent increase in the presence of HEWL fibrils along with a blue shift of the emission maximum from 477 nm suggesting the complexation of ANS with exposed hydrophobic patches of HEWL. (Fig. 6). The addition of COR to HEWL resulted in a drastic reduction in ANS fluorescence intensity (Fig. 6) indicating that under fibrillation conditions COR could efficiently inhibit the exposure of buried hydrophobic patches of HEWL via stabilization of the native HEWL structure. This large fluorescence decrease is indicative of the inhibition of exposure of large buried hydrophobic patches on the surface of HEWL in the presence of COR. As the exposure of accessible non-polar surface area of HEWL is an essential step in the fibrillogenesis process so a significant reduction in the extent of exposure of the hydrophobic regions in presence of COR suggested that COR could efficiently arrest the HEWL fibrillogenesis.

Intrinsic Fluorescence Studies

To decipher the influence of COR on the conformation of HEWL upon fibrillation the intrinsic fluorescence of HEWL in the absence as well as presence of COR was monitored. The fluorophores in HEWL are sensitive to their microenvironmental polarity. TRP residues 62 and 63 of HEWL being positioned in the amyloid prone region are consequently involved in the fibrillation process. Hence, by investigating the fluorescence changes in these residues we can gain insights into various aspects of the fibrillation process.[94] The HEWL samples exhibit an emission maximum at 338 nm when excited at 295 nm.[27] During fibrillation there is unfolding of HEWL which

REVISED MANUSCRIPT

changes the microenvironment of the initially buried TRP moieties from a hydrophobic environment to a more hydrophilic one (exposure to bulk aqueous acidic buffer solution) resulting in quenching of intrinsic fluorescence intensity of the fibrillar HEWL samples in comparison to native HEWL. With the onset of the fibrillogenesis process there was a marked reduction in the fluorescence of the HEWL samples. A plot of the normalized fluorescence of HEWL samples both in the absence and presence of COR at the emission maxima (338 nm) against time is shown in Fig. 7. Such drastic alterations in TRP fluorescence are indicative of changes in the tertiary structure of HEWL upon fibrillation. Since the fluorescence quantum yield of TRP is less in a polar environment than in a non-polar one so the decrease in fluorescence suggests that the TRP residues are exposed from a

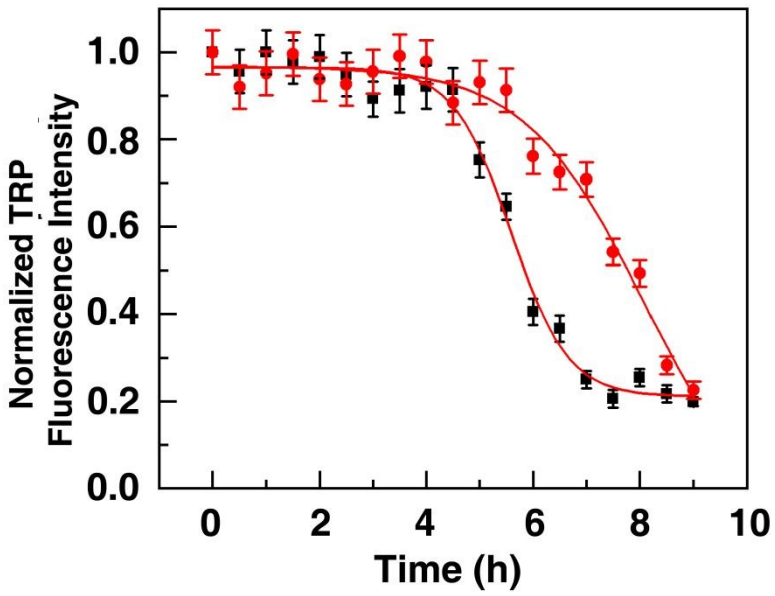

Fig. 7. Variation of the intrinsic fluorescence intensity of HEWL samples at the emission maxima with time in the absence (■) and presence (•) of COR.

hydrophobic to a more hydrophilic (aqueous acidic buffer) environment during fibrillogenesis. The TRP fluorescence can also be quenched by the different

neighboring amino acid residues through various quenching mechanisms.[95-99] Such quenching interactions result from the intra/intermolecular interactions of the TRP residues with its surrounding amino acids present within the fibrillar network of HEWL.[100] This indicates that the local environment of the tryptophan residues in the HEWL fibril has become more accessible to aqueous solvent during the process of fibril formation, resulting in the quenching of fluorescence by water.[101,102] The change in intrinsic fluorescence of HEWL samples was delayed upon addition of COR. This indicated that the changes in the local environment surrounding the TRP residues were arrested/delayed in presence of COR. Since the drop in intrinsic fluorescence of HEWL is associated with the exposure of the TRP residues to a more hydrophilic aqueous acidic environment so we can conclude that the microenvironmental changes of the initially buried TRP residues during fibrillogenesis of HEWL were delayed upon addition of COR. Thus, the intrinsic fluorescence studies indicated that COR retarded fibrillation in HEWL which further reinstates the observations from ThT fluorescence and CR absorbance assays.

Anisotropy Studies. Steady-state fluorescence anisotropy experiments can be employed to monitor the aggregation behavior of HEWL.[103,104] So, the steady-state TRP fluorescence anisotropy measurements were performed to study the fibrillation in HEWL both in the absence and presence of COR. Variations in the anisotropy behavior of HEWL samples before and after fibrillation in aqueous acidic buffer was monitored using steady state anisotropy experiments. The anisotropy values of HEWL increased upon fibrillation which indicated that the local environment surrounding the TRP residues became more compact which restricted the motion of

View Article Online
DOI: 10.1039/D1NJ06007D

TRP residues leading to an enhancement in fluorescence anisotropy. However, in the presence of COR, the relative increase in the anisotropy value was decreased from (0.216±0.003) to (0.174±0.003). Thus, COR affected a by ~19.44% reduction in the anisotropy value which suggested that the extent of fibrillation in HEWL was suppressed by COR. Thus, fibrillation in HEWL proceeds with burial of the TRP residues into a more compact environment, which is mitigated to an extent by COR highlighting its ability to suppress HEWL fibrillation.

CD studies

CD is a useful tool widely used in protein chemistry. Far UV CD spectroscopy was employed to investigate the secondary structural changes in HEWL upon fibrillation in absence as well as presence of COR. When amyloid fibrils are generated,

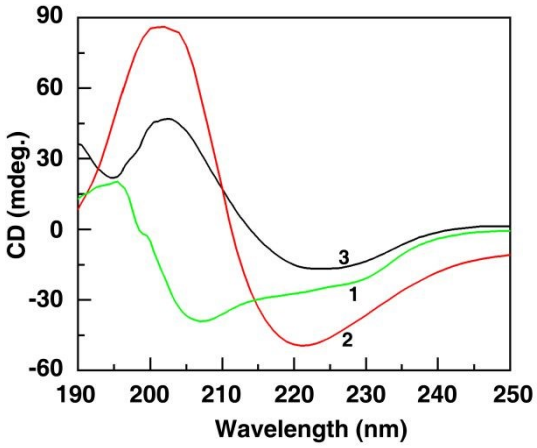

Fig. 8. Far-UV CD spectral changes of HEWL samples upon fibrillation. Curve 1 represents the far-UV CD spectrum of HEWL before fibrillation while curves 2 and 3 represent the CD spectrum of HEWL samples after fibrillation in the absence and presence of COR, respectively.

there is a marked increase in the β-sheet content of proteins/peptides. To study the effect of COR on the secondary structural changes induced in HEWL upon fibrillation the far-UV CD spectra of HEWL in the absence and presence of COR

were recorded and subsequently analyzed. The changes in the far UV CD spectra of HEWL upon fibrillation both in the absence and presence of COR are depicted in Fig. 8. The far UV CD spectra of HEWL showed α-rich conformation (~35.90% α-helix, ~15.10% β-sheet, ~49% turns and unordered) which was characterized by minimum at ~208 nm and a negative shoulder at ~222 nm before the advent of fibrillation (with or without COR)[22,105,106] With increase in time there was a structural transition in HEWL which caused a prominent shift in its secondary structure to an extremely amyloidogenic but soluble β-sheet rich structure.[22,72,106] After 9 h the CD spectrum of HEWL showed a marked change and was characterized by a well defined minimum at 221 nm. This is characteristic of the β-sheet rich

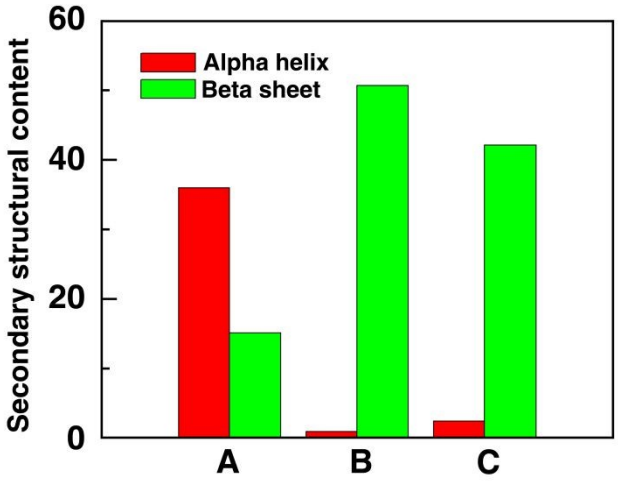

Fig. 9. Changes in the α-helical and β-sheet content of HEWL before (A) and after fibrillation both in the (B) absence and (C) presence of COR.

conformation (~0.90% α-helix, ~50.70% β-sheet, ~48.40% turns and unordered). HEWL samples treated with COR after 9 h also exhibited a minimum at ~222 nm but upon deconvolution of the CD spectrum there was a noticeable decrease in the β-sheet content (~2.40% α-helix, ~42.10% β-sheet, ~55.50% turns and unordered) of HEWL. The changes in the α-helical and β-sheet content of HEWL before and after

REVISED MANUSCRIPT

fibrillation both in the presence and absence of COR are presented in Fig. 9. These observations unequivocally state that COR arrests α to β structural transition in HEWL yielding less β-sheet structure but the original α-helical structure in native HEWL was not restored. There was an increase in the proportion of turn and unordered structures in HEWL. Thus, the CD results suggested that the increase in β-sheet content and concomitant α-to-β transition of HEWL, which is the hallmark of amyloid fibrillation, was successfully attenuated by COR which reinstate our earlier observations from ThT fluorescence.

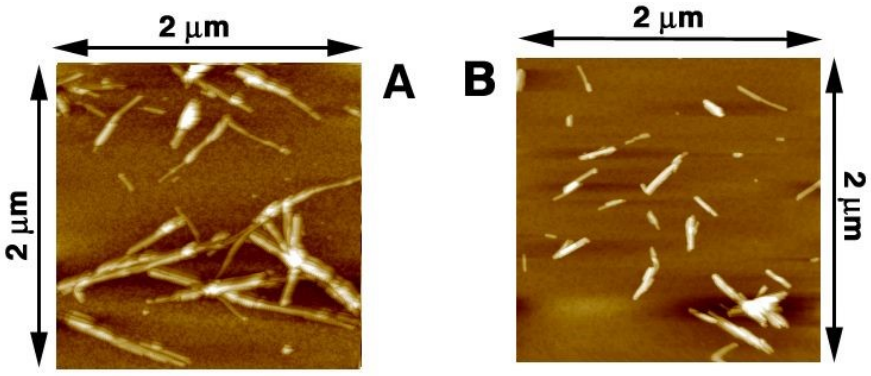

Fig. 10. AFM images of HEWL fibrils in the absence (A) and presence (B) of COR after 9 h.

AFM imaging

To examine the fibril attenuating of COR in more details AFM was performed. AFM enabled us to study the morphological characteristics of HEWL samples both in the absence and presence of COR. Fig. 10A clearly revealed that after 9 h large amount of thickly populated, compact, elongated and matured fibrillar assemblies were formed. These elongated, dense and matured fibrillar aggregates are the characteristic of amyloid fibrils. On the other hand Fig. 10B showed that upon addition of COR HEWL fibrillogenesis was markedly inhibited. On treatment with COR the fibrils became less dense, fragmented, sparsely populated and resembled

the protofibrillar structures. The HEWL fibrils were not only highly scattered and lesser in quantity but significantly less matured/developed and their morphology was also altered in presence of COR. The figures also confirm that the growth of fibrillar assemblies was significantly disrupted by COR. Thus, AFM studies reaffirmed COR inhibited fibrillogenesis in HEWL remarkably. Thus AFM imaging conclusively indicate that treatment of HEWL samples with COR suppresses amyloid fibril formation efficiently. The spectroscopic assays in conjunction with the imaging experiments conclusively establish that exposure of HEWL to COR causes bona fide retardation/inhibition of amyloid fibrillation.

DSC studies. Alkaloids on complexation with proteins can affect their thermal stability which is manifested by changes in their thermal denaturation temperature. DSC is a microcalorimetric tool to detect any such alterations in the thermal stabilities of proteins. Additionally, it also provides insights into the energetics associated with the thermal denaturation process. Effect of COR on the thermal stability of HEWL was monitored using DSC. The DSC thermogram of HEWL exhibited a single endothermic peak at (331.77 ± 0.03) K (Fig. S2, curve 1). In presence of COR the peak in the thermogram remained virtually unaltered at (332.09 ± 0.05) K (Fig. S2, curve 2). So COR did not affect any significant change in the melting temperature of HEWL suggesting that the HEWL-COR complexation under amyloidogenic buffer conditions did not alter its thermal stability which in turn implies that the structural integrity of native HEWL was retained in presence of COR. Furthermore, there was no alteration in the shape of the thermograms in presence of COR indicating that COR did not affect the thermal denaturation pathway of HEWL. The transitional enthalpy of HEWL (ΔH_{cal}) enhanced

from (65.05 ± 0.58) to (94.52 ± 0.13) kcal/mol in presence of COR. Overall, we can say that in presence of COR the thermal denaturation process of HEWL at pH 2.20 was not affected significantly which can be linked to the fibril attenuating potential of COR and its ability to resist the conformational changes in native HEWL.

ITC Studies

The binding reaction between COR and HEWL under amyloidogenic buffer conditions was characterized by ITC. ITC is the most efficient tool for characterizing the binding thermodynamics of a biomolecular interaction process. The ITC thermogram for the complexation of HEWL with COR at 25 ^{o}C is presented in Fig. 11. Analysis of the ITC thermogram after appropriate correction for the heats of dilution using one set of site binding model afforded the equilibrium constant (K), binding stoichiometry (N) and standard molar enthalpy contribution (ΔH^0). The K value for COR-HEWL complexation was deduced to be (6.41 ± 0.46) × 10^4 M^{-1} while the N value was found to be (1.13 ± 0.02) suggesting 1 : 1 association between HEWL and COR. The complexation was favored by negative ΔH^0 value of (-4.37 ± 0.04) kcal/mol which mainly originated from the restricted mobility of COR molecules entrapped in the low dielectric interior of HEWL. The standard molar Gibbs energy (ΔG^0) and the entropic contributions ($T\Delta S^0$, where T is the absolute temperature and ΔS^0 is the standard molar entropy change) to the binding were calculated using the relationships $\Delta G^0 = -RT \ln(K)$ and $\Delta G^0 = \Delta H^0 - T\Delta S^0$, respectively.

View Article Online
DOI: 10.1039/D1NJ06007D

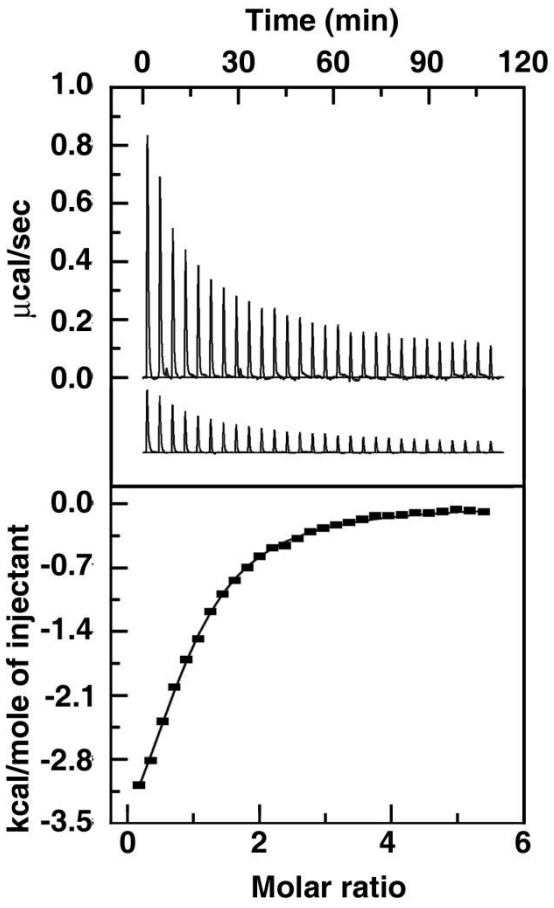

Fig. 11. The upper panel represents the ITC thermogram for COR-HEWL complexation at 298.15 K (curve on the top), along with the dilution profile (curve at the bottom offset for clarity). The bottom panel shows the integrated heat data after correction of heat of dilution. The symbols (■) represent the data points and the solid line represents the best-fit data.

The value of ΔG^0 and $T\Delta S^0$ for HEWL-COR binding was calculated to be (-6.56 ± 0.46) and (2.19 ± 0.42) kcal/mol, respectively. The negative ΔG^0 value accounts for the spontaneity of HEWL-COR complexation under fibrillogenic buffer conditions. The positive $T\Delta S^0$ arises due to the release of condensed counterions and changes in the HEWL hydration layers consequent to the COR binding.

Molecular docking

In silico molecular docking was used to study for further investigating the binding interaction between HEWL and COR. The conformational cluster analysis of 50 runs

was performed using RMSD tolerance of 2.0 Å and the lowest energy with most populated conformation was utilized for investigating the binding details as shown in Fig. 12. The value of Gibbs free energy ($\Delta G°$) of binding for the best conformation with the lowest energy was found -7.61 kcal/mol. The sum of van der Waal's energy, hydrogen bond energy and desolvation energy was -8.71 kcal/mol and the electrostatic energy was -0.09 kcal/mol which were added to obtain the value of the total intermolecular energy (ΔE_1 = -8.81 kcal/mol). There were 4 active torsions between C2_3 and O1_2, C11_13 and O2_14, C13_16 and O3_17, C21_25 and O4_26 which contributed to the torsional free energy (ΔE_3) of +1.19 kcal/mol. The internal energy (ΔE_2) and the unbound system's energy (ΔE_4) afforded the same value of -0.48 kcal/mol (Table 1). In the interaction cavity of HEWL, some amino acid residues are present and are involved in hydrophobic interactions like VAL109, GLU35, ASN59, ILE58, ILE98, LEU75, TRP63 as shown in Fig. 13. However, that doesn't indicate that the interaction of COR with HEWL protein is exclusively hydrophobic. There were some polar interactions also like π-σ (TRP108), π-π stacked, π-π T shaped (TRP62) and carbon hydrogen bonding (ASP101, GLN57, LEU56, ALA107). These polar interactions had played a significant role in the stability of the COR-HEWL binding interaction.

View Article Online
DOI: 10.1039/D1NJ06007D

Table 1. Evaluated docking energies with possible binding sites of COR in HEWL.

Energy (kcal/mol)	Site I	Site II	Site III
$\Delta G°$	-7.61	-7.58	-6.37
ΔE_1 (a+b)[a]	(-8.71)+(-0.09)	(-8.65)+(-0.13)	(-7.33)+(-0.24)
ΔE_2	-0.48	-0.72	-0.71
ΔE_3	+1.19	+1.19	+1.19
ΔE_4	-0.48	-0.72	-0.71

[a]where a = van der Waal's energy+ hydrogen bond energy + desolvation energy; b = electrostatic energy.

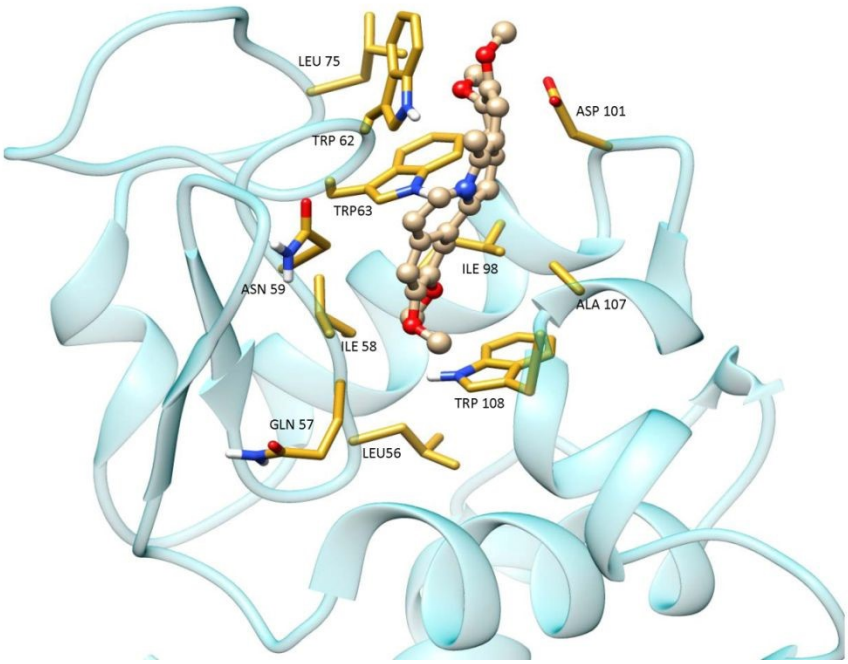

Fig. 12. 3D image of the lowest energy conformer of COR (ball and stick form) on HEWL with hydrophobic amino acid residues marked with golden colour (site I).

View Article Online
DOI: 10.1039/D1NJ06007D

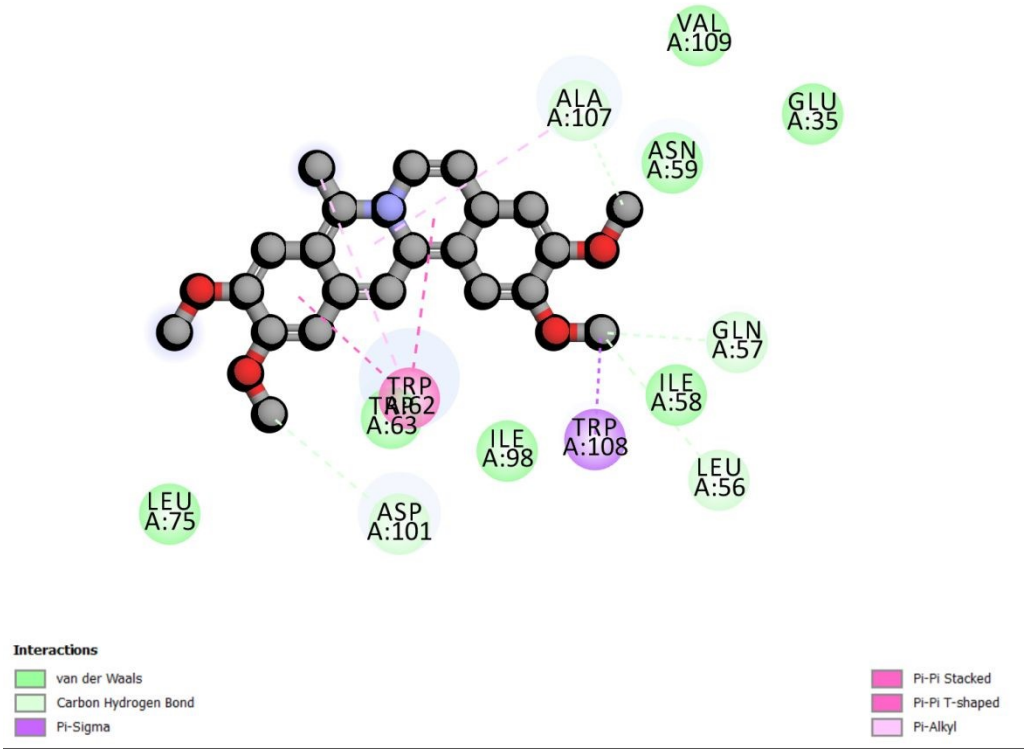

Fig. 13. 2D image of conformation displaying interactions with amino acid residues.

The change in the value of ASA of the residues (*i*), which depends on its accessibility to the solvent were calculated for HEWL and HEWL-COR complex were calculated using the following equation:

$$\Delta\mathbf{ASA}^{i} = \Delta\mathbf{ASA}^{i}{}_{HEWL} - \Delta\mathbf{ASA}^{i}{}_{HEWL\text{-}COR} \qquad (3)$$

Total ASA of native HEWL (1dpx) was 6313.746Å^2 while upon complexation with COR it declined to 6178.86Å^2 (Fig 14). The substantial decrease in the value of ASA of HEWL complexed with COR in respect of ASA of native HEWL provides important information about the binding interaction. The amino acid residues with ASA difference of >10Å^2 in between native HEWL and complexed HEWL are considered to have effective and significant role in the binding mechanism. Such amino acid residues which show a decrease in ASA value greater than 10Å^2 are

View Article Online
DOI: 10.1039/D1NJ06007D

enlisted in Table 2. Among all these amino acid residues, TRP-62 showed the highest decrease of 74.371Å^2 in ASA after binding with COR due to π-π stacked & π-π T shaped interactions. Some other amino acids such as ALA-107, ASP-101, ASN-59 and TRP-63 also shows reduction in the value of ASA in HEWL.

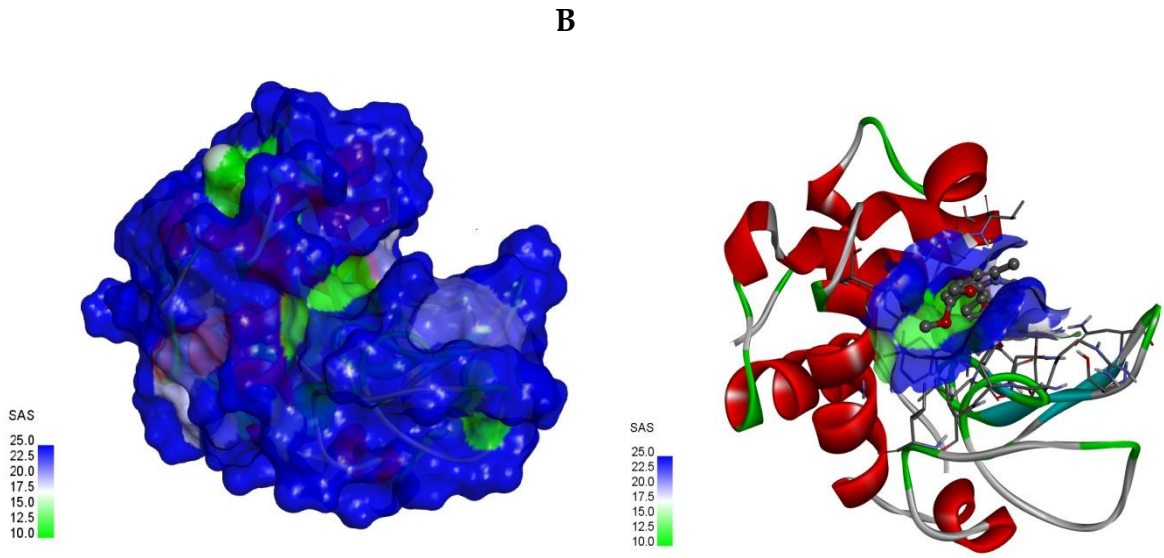

Fig 14. Solvent-accessible surface area of (A) native HEWL and of (B) HEWL complexed with COR.

View Article Online
DOI: 10.1039/D1NJ06007D

Table 2. Changes in the ASA (Å^2) values of the interacting residues of HEWL before and after binding with COR.

System	Residues	ASA(Å^2) in HEWL	ASA(Å^2) in complex	ΔASA (Å^2)
HEWL-COR	GLU-35	31.959	26.186	5.773
	LEU-56	0.00	0.00	0.00
	GLN-59	11.920	3.183	8.737
	ILE-58	2.383	0.113	2.27
	ASN-59	28.724	0.871	27.853
	TRP-62	135.967	61.596	74.371
	TRP-63	23.466	4.874	18.592
	LEU-75	78.280	68.180	10.10
	ILE-98	7.583	1.001	6.582
	ASP-101	100.565	65.887	34.678
	ALA-107	53.977	13.302	40.675
	TRP-108	10.919	0.000	10.919
	VAL-109	96.281	88.976	7.305

Mechanistic Insights

Our results suggested that nucleation as well as fibril growth were efficiently inhibited by COR. COR interacted with HEWL at very low (μM) concentration directly in a site-specific manner and arrested exposure of the partially unfolded HEWL surface which in turn, caused concomitant inhibition of self-association and amyloid fibrillation. In the presence of COR there is a possibility of interaction through preferential hydration of the HEWL surface.[107] However, COR did not cause refolding of HEWL into its native state

which suggests that COR binds with the partially unfolded HEWL and thereby leads to suppression of formation of amyloid fibrils. Under the highly acidic experimental conditions COR which has a planar extended π molecular framework can bind with HEWL through a multitude of forces like π-π stacking, hydrophobic interactions, etc. which inhibit the fusion of HEWL molecules and inhibits the formation of fibrillar assemblies.[82] Previous reports demonstrated that the active hydroxyl groups of polyphenols play a major role in the inhibition of fibrillation.[104,108-110] Although no such active hydroxyl groups are present in COR but it is highly likely the methoxy groups present in COR play a major part in its inhibitory influence on fibrillogenesis through their involvement in multiple hydrophobic interactions with partially unfolded HEWL. HEWL denaturation opens up the binding sites for interaction with COR and this interaction prevents amyloid fibrillation through the intercalation of smaller fibrils to generate larger fibrillar assemblies.

Conclusions

This paper describes the influence of the protoberberine alkaloid COR on HEWL amyloidogenesis. In the presence of COR the formation of fibrillar assemblies in HEWL was markedly delayed as revealed by monitoring the fibrillation kinetics through ThT fluorescence assay. CR assay in absorbance also reiterated that COR had a significant inhibitory effect on the fibrillation process. The margin of fibrillation was also remarkably suppressed in the presence of this protoberberine alkaloid. NR assay indicated that COR exerted an inhibitory effect on the tertiary structural changes in HEWL which also pointed towards its fibrillation inhibitory propensity. ANS assay showed that the exposure of the buried non-polar regions

associated with fibrillation was suppressed by COR. The changes associated with the microenvironmental polarity and the steady state anisotropy of the TRP residues present in HEWL due to fibrillation were delayed as well as arrested in presence of COR. Far UV CD experiments indicated that α to β transitions in HEWL which is the hallmark of fibrillogenesis was efficiently suppressed by COR and the β sheet content of HEWL was reduced upon addition of COR. The imaging studies also testified that the amyloid fibrillation was remarkably inhibited by COR. DSC studies showed that COR did not alter the thermal denaturation process of HEWL under amyloidogenic buffer conditions significantly. The complete thermodynamic profile for HEWL-COR binding along with the equilibrium constant and binding stoichiometry was also evaluated with the help of ITC. Molecular docking analysis provided further insights into the nature of interactions between HEWL and COR. All these experiments unequivocally establish that COR can effectively arrest fibrillogenesis at very low concentrations (in μM range). Hence, such protoberberine alkaloids can be used for designing viable therapeutics for effective treatment of amyloidosis and other ailments related to protein aggregation.

Conflicts of interest

There are no conflicts of interest to declare.

Acknowledgements

AB acknowledges the financial assistance from Department of Science and Technology and Biotechnology, Govt. of West Bengal project (GO No.: 32(Sanc.)-ST/P/S&T/15G-13/2018 dated 31.01.2019) and also the DST FIST grant (Sanction letter No. SR/FST/CS-I/2017/7(C) dated December 28, 2018).

References

(1) C. M. Dobson, *Semin. Cell Dev. Biol.,* 2004, **15**, 3–16.

(2) S. S. S. Wang and T. A. Good, *J. Chin.Inst. Chem. Eng.,* 2005, **36**, 533–559.

(3) P. P. Liberski, B. Sikorska, J. J. Hauw, N. Kopp and N. Streichenberger, et al. *Ultrastruct. Pathol.,* 2010, **34**, 351-361.

(4) D. B. Kell, *Arch. Toxicol.,* 2010, **84**, 825–889

(5) J. W. Wu, K. -N. Liu, S. -C. How, W. -A. Chen, C. -M. Lai, et al. *PLoS ONE,* 2013, *8*, e81982.

(6) M. Sunde and C. Blake, *Adv. Protein Chem.,* 1997, **50**, 123-159.

(7) A. Trovato, F. Chiti, A. Maritan, and F. Seno, *PLoS Comput. Biol.,* 2006, **2**, 1608-1618.

(8) C. Iannuzzi, R. Maritato, G. Irace and I. Sirangelo, *Int. J. Mol. Sci.,* 2013, **14**, 14287-14300.

(9) M. Stefani, and C. M. Dobson, *J. Mol. Med.,* 2003, **81**, 678-699.

(10) S. J. C. Lee, E. Nam, H. J. Lee, M. G. Savelieff and M. H. Lim, *Chem. Soc. Rev.,* 2017, **46**, 310323.

(11) A. C. Bhasikuttan and J. Mohanty, Detection, *Chem. Commun.,* 2017, **53**, 2789-2809.

(12) F. Chiti and C. M. Dobson, *Annu. Rev. Biochem.,* 2006, **75**, 333–366.

(13) A. M. Palmer, *Trends Pharmacol. Sci.,* 2011, **32**, 141-147.

(14) F. E. Cohen and J. W. Kelly, *Nature,* 2003, **426**, 905-909.

(15) E. Gazit, *FEBS J.,* 2005, **272,** 5971-5978.

(16) C. M. Dobson, *Nature,* 2003, **426**, 884–890.

(17) T. R. Jahn and S. E. Radford, *FEBS J.,* 2005, **272**, 5962–5970.

(18) T. Cohen, A. Frydman-Marom, M. Rechter and E. Gazit, *Biochemistry,* 2006, **45**, 4727–4735.

(19) F. G. De Felice, M. N. N. Vieira, L. M. Saraiva, J. D. Figueroa-Villar, J. Garcia-Abreu, R. Liu, L. Chang, W. L. Klein and S. T. Ferreira, *FASEB J.,* 2004, **18**, 1366–1372.

(20) M. Masuda, N. Suzuki, S. Taniguchi, T. Oikawa, T. Nonaka, T. Iwatsubo, S. Hisanaga, M. Goedert and M. Hasegawa, *Biochemistry,* 2006, **45**, 6085–6094.

(21) M. N. N. Vieira, J. D. Figueroa-Villar, M. N. L. Meirelles, S. T. Ferreira and F. G. De Felice, *Cell Biochem. Biophys.,* 2006, **44**, 549–553.

(22) S. -C. How, S. -M. Yang, A. Hsin, C. -P. Tseng, S. -S. Hsueh, M. -S. Lin, R. P. -Y. Chen, W. -L. Chou and S. S. -S. Wang, *Food Funct.,* 2016, **7**, 4898-4907.

(23) B. Masschalck and C. W. Michiels, *Crit. Rev. Microbiol.,* 2003, **29**, 191-214.

(24) Ç. Mecitoglu, A. Yemenicioglu, A. Arslanoglu, Z. S. Elmaci, F. Korel and A. E. Çetin, *Food Res. Int.,* 2006, **39**, 12-21.

(25) M. Buck, H. Schwalbe and C. M. Dobson, *Biochemistry,* 1995, **34**, 13219-13232.

(26) A. Ghosh, K. V. Brinda and S. Vishveahwara, *Biophys. J.*, 2007, **92**, 2523-2535.

(27) Z. R. Zhang, Q. Zheng, J. Han, G. P. Gao, J. Liu and T. Gong, *Biomaterials,* 2009, **30**, 1372-1381.

(28) Z. Gu, X. Zhu, S. Ni, Z. Su and H. M. Zhou, *Int. J. Biochem. Cell Biol.,* 2004, **36**, 795-805.

(29) A. Das, R. Thakur, A. Dagar and A. Chakraborty, *Phys. Chem. Chem. Phys.,* 2014, **16**, 5368-5381.

(30) Y. Fang, L. Yi, and Y. Fang, *Acta Chim. Sin.*, 2003, **61**, 803-807.

(31) N. C. J. Strynadka and M. N. G. James, *J. Mol. Biol.*, 1991, **220**, 401-424.

(32) C. C. Blake, D. F. Koenig, G. A. Mair, A. C. North, D. C. Phillips and V. R. Sarma, *Nature,* 1965, **206**, 757-761.

(33) B. Gatto, M. M. Sanders, C. Yu, H. Y. Wu, D. Makhey, E. J. LaVoie and L. F. Liu, *Cancer Res.,* 1996, **56**, 2795–2800.

(34) L. K. Wang, B. D. Rogers and S. M. Hecht, *Chem. Res. Toxicol.,* 1996, **9**, 75–83.

(35) D. Makhey, B. Gatto, C. Yu, A. Liu, L. F. Liu, E. J. LaVoie, *Bioorg. Med. Chem.,* 1996, **4**, 781–791.

(36) D. S. Pilch, C. Yu, D. Makhey, E. J. LaVoie, A. R. Srinivasan, W. K. Olson, R. R. Sauers, K. J. Breslauer, N. E. Geacintov and L. F. Liu, *Biochemistry,* 1997, **36**, 12542–12553.

(37) D. S. Phillips and R. N. Castle, *J. Heterocycl. Chem.,* 1988, **18**, 223–232.

(38) S. Pal, G. Suresh Kumar, D. Debnath and M. Maiti, *Indian J. Biochem. Biophys.,* 1998, **35**, 321–332.

(39) S. Pal, S. Das, G. Suresh Kumar and M. Maiti, *Curr. Sci.,* 1998, **75**, 496–500.

(40) J. S. Lee, L. J. Latimer and K. J. Hampel, *Biochemistry,* 1993, **32**, 5591–5597.

(41) A. A. Moraru-Allen, S. Cassidy, J. L. Asensio Alvarez, K. R. Fox, T. Brown and A. N. Lane, *Nucleic Acids Res.,* 1997, **25**, 1890–1896.

(42) O. Persil, C. T. Santai, S. S. Jain and N. V. Hud, *J. Am. Chem. Soc.,* 2004, **126**, 8644–8645.

(43) F. Xing, G. Song, J. Ren, J.B. Chaires and X. Qu, *FEBS Lett.,* 2005, **579**, 5035–5039.

(44) P. Giri and Suresh Kumar, G. *Mol. BioSyst.,* 2008, **4**, 341–348.

(45) H. Ihmels and A. Salbach, *Photochem. Photobiol.,* 2006, **82**, 1572–1576.

(46) K. Bhadra and G. Suresh Kumar, *Biochim. Biophys. Acta,* 2008**, 1780**, 298–306.

(47) M. M. Islam and G. Suresh Kumar, *Biochim. Biophys. Acta,* 2009, **1790**, 829–839.

(48) M. M. Islam, S. Roy Chowdhury and G. Suresh Kumar, *J. Phys. Chem. B,* 2009, **113**, 1210-1224.

(49) R. Sinha and G. Suresh Kumar, *J. Phys. Chem. B,* 2009, **113**, 13410–13420.

(50) M. M. Islam, P. Pandya, S. Kumar and G. Suresh Kumar, *Mol. BioSyst.,* 2009, **5**, 244–254.

(51) K. Bhadra and G. Suresh Kumar, *Biochim. Biophys. Acta,* 2011, **1810**, 485–496.

(52) A. Basu and G. Suresh Kumar, *J. Chem. Thermodyn.,* 2016, **101**, 221–226.

(53) G. Suresh Kumar and A. Basu, *Biochim. Biophys. Acta,* 2016, **1860**, 930–944.

(54) A. Basu and G. Suresh Kumar, *Biochim. Biophys. Acta,* 2018, **1862**, 1995–2016.

(55) D. R. Booth, M. Sunde, V. Bellotti, C. V. Robinson, W. L. Hutchinson, P. E. Fraser, P. N. Hawkins, C. M. Dobson, S. E. Radford, C. C. F. Blake and M. B. Pepys, *Nature,* 1997, **385**, 787–793.

(56) M. B. Pepys, P. N. Hawkins, D. R. Booth, D. M. Vigushin, G. A. Tennent, A. K. Soutar, N. Totty, O. Nguyen, C. C. Blake and C. J. Terry, et al. *Nature,* 1993, **362**, 553–557.

(57) R. H. C. Strang, *Biochem. Educ.*, 1984, **12**,57-59.

(58) A. Kroes-Nijboer, P. Venema, J. Bouman and E. van der Linden, *Langmuir,* 2011, **27**, 5753–5761.

(59) L. Nielsen, R. Khurana, A. Coats, S. Frokjaer, J. Brange, S. Vyas, V. N. Uversky and A. L. Fink, *Biochemistry,* 2001, **40**, 6036–6046.

(60) N. Darghal, A. Garnier-Suillerot and M. Salerno, *Biochem. Biophys. Res.Commun.,* 2006, **343**, 623–629.

(61) S. W. Provencher and J. Glockner, *Biochemistry*, 1981, **20**, 33–37.

(62) I. H. M. Van Stokkum, H. J. W. Spoelder, M. Bloemendal, R. Van Grondelle and F .C. A. Groen, *Anal. Biochem.*, 1990, **191**, 110–118.

(63) N. Sreerama and R. W. Woody, *Anal. Biochem.*, 2000, **287**, 252–260.

(64) L. Whitmore and B. A. Wallace, *Nucleic Acids Res.*, 2004, **32**, W668-W673.

(65) L. Whitmore and B. A. Wallace, *Biopolymers*, 2008, **89**, 392-400.

(66) A. Basu and G. Suresh Kumar, *J. Agric. Food Chem.*, 2014, **62**, 7955−7962.

(67) A. Basu and G. Suresh Kumar, *Food Funct.*, 2014, **5**, 1949-1955.

(68) A. Basu and G. Suresh Kumar, *J. Hazard. Mater.,* 2014, **273**, 200-206.

(69) A. Basu and G. Suresh Kumar, *Food Chem.,* **2015**, **175**, 137-142.

(70) A. Basu and G. Suresh Kumar, *J. Chem. Thermodyn.,* 2016, **100**, 100-105.

(71) A. Basu and G. Suresh Kumar, *J. Phys. Chem. B,* 2017, **121**, 1222–1239.

(72) A. Basu and G. Suresh Kumar, *Mol. BioSyst.,* 2017, **13**, 1552-1564.

(73) A. Basu and G. Suresh Kumar, *J. Chem. Thermodyn.,* 2018, **126**, 91-96.

(74) E. Kobayashi, K. Yura and Y. Nagai, *Biophysics*, 2013, **9**, 1-12.

(75) J. Zhang, W. Chen, B. Tang, W. Zhang, L. Chen, Y. Duan, Y. Zhu, Y. Zhu and Y. Zhang, *RSC Adv.,* 2016, **6**, 23622-23633.

(76) P. S. Vassar and C. F. A. Culling, *Arch. Pathol.,* 1959, **68**, 487–498.

(77) H. R. Kalhor, M. Kamizi, J. Akbari and A. Heydari, *Biomacromolecules*, 2009, **10**, 2468–2475.

(78) S. S. -S. Wang, K. N. Liu, B. W. Wang, *Eur. Biophys. J.,* 2010, **39**, 1229–1242.

(79) S. S. -S. Wang, Y. T. Hung, W. S. Wen, K. C. Lin and G. Y. Chen, *Biochim. Biophys. Acta Mol. Cell Biol. Lipids,* 2011, **1811**, 301-313.

(80) J. D. Harper and P. T. Lansbury Jr., *Annu. Rev. Biochem.,* 1997, **66**, 385–407.

(81) M. Bartolini, C. Bertucci, M. L. Bolognesi, A. Cavalli, C. Melchiorre and V. Andrisano, *ChemBioChem,* **2007**, **8**, 2152–2161.

(82) S. Bag, R. Mitra, S. Dasgupta and S. Dasgupta, *J. Phys. Chem. B,* 2017, **121**, 5474-5482.

(83) Y. Kumar, S. Tayyab and S. Muzammil, *Arch. Biochem. Biophys.,* 2004, **426**, 3-10.

(84) I. Nasir, M. Lundqvist and C. Cabaleiro-Lago, *Nanoscale,* 2015, **7**, 17504-17515.

(85) P. Ladewig, *Nature*, 1945, **156**, 81–82.

(86) W. G. Turnell and J. T. Finch, *J. Mol. Biol.,* 1992, **227**, 1205-1223.

(87) W. E. Klunk, R. F. Jacob and R. P. Mason, *Methods Enzymol.,* 1999, **309**, 285-305.

(88) A. V. Terry and J. Buccafusco, *J. Pharmacol. Exp. Ther.,* 2003, **306**, 821–827.

(89) G. V. Semisotnov, N. A. Rodionova, O. I. Razgulyaev, V. N. Uversky, A. F. Gripas and R. I. Gilmanshin, *Biopolymers,* 1991, **31**, 119–128.

(90) X. Chong, L. Sun, Y. Sun, L. Chang, A. K. Chang, X. Lu, X. Zhou, J. Liu, B. Zhang, G. W. Jones and J. He, *Int. J. Biol. Macromol.,* 2017, **101**, 321–325.

(91) B. Bolognesi, J. R. Kumita, T. P. Barros, E. K. Esbjorner, L. M. Luheshi, D. C. Crowther, M. R. Wilson, C. M. Dobson, G. Favrin and J. J. Yerbury, *ACS Chem. Biol.*, 2010, **5**, 735-740.

(92) S. K. Chaturvedi, P. Alam, J. M. Khan, M. K. Siddiqui, P. Kalaiarasan, N. Subbarao, Z. Ahmad and R. H. Khan, *Int. J. Biol. Macromol.*, 2015, **80**, 375-384.

(93) G. Sancataldo, V. Vetri, V. Foderà, G. Di Cara, V. Militello and M. Leone, *PLoS One,* 2014, **9**, e84552.

(94) E. Frare, P. P. De Laureto, J. Zurdo, C. M. Dobson and A. Fontana, *J. Mol. Biol.*, 2004, **340**, 1153-1165.

(95) M. Rholam, S. Scarlata and G. Weber, *Biochemistry,* 1984, **23**, 6793–6796.

(96) M. Eftink, *Methods Biochem. Anal.*, 1991, **35**, 127–205.

(97) Y. Chen and M. Barkley, *Biochemistry,* 1998, **37**, 9976–9982.

(98) J. Vivian and P. Callis, *Biophys. J.*, 2001, **80**, 2093-2109.

(99) Chaari, A.; C. Fahy, A. Chevillot-Biraud and M. Rholam, *PLoS ONE,* 2015, **10**, e0142095.

(100) E. Nishimoto, S. Yamashita, A. Szabo, and T. Imoto, *Biochemistry* **1998**, *37*, 5599-5607.

(101) C. Duy and J. Fitter, *Biophys. J.*, 2006, **90**, 3704–3711.

(102) K. Russo, E. Di Stasio, G. Macchia, G. Rosa, A. Brancaccio and T. C. Petrucci, *Biochem. Biophys. Res. Commun.*, 2000, **274**, 93–98.

(103) J. R. Lakowicz, Principles of Fluorescence Spectroscopy, 3rd ed., Kluwer Academic/Plenum Publishers, New York, Boston, Dordrecht, London, Moscow, 2009, pp. 353–370.

(104) S. Bhattacharya, N. K. Pandey, A. Roy and S. Dasgupta, *Int. J. Biol. Macromol.*, 2014, **70**, 312-319.

(105) C. Jash and G. Suresh Kumar, *RSC Adv.*, 2014, **4**, 12514-12525.

(106) A. Basu, S. C. Bhattacharya and G. Suresh Kumar, *Int. J. Biol. Macromol.*, 2018, **107**, 2643–2649.

(107) S. Choudhary, N. Kishore and R. V. Hosur, *Sci. Rep.*, 2015, **5**, 17599.

(108) Y. Porat, A. Abramowitz and E. Gazit, *Chem. Biol. Drug Des.*, 2006, **67**, 27-37.

(109) Q. I. Churches, J. Caine, K. Cavanagh, V. C. Epa, L. Waddington, C. E. Tranberg, A. G. Meyer, J. N. Varghese, V. Streltsov and P. J. Duggan, *Bioorg. Med. Chem. Lett.*, 2014, **24**, 3108-3112.

(110) M. S. Borana, Pushpa Mishra, R. R. S. Pissurlenkar, R. V. Hosur, B. Ahmad, *Biochim. Biophys. Acta*, 2014, **1844**, 670–680.

REVISED MANUSCRIPT